

Imaging characteristics of tenosynovial and bursal chondromatosis

Eric A. Walker · Mark D. Murphey · John F. Fetsch

Received: 19 April 2010 / Revised: 15 July 2010 / Accepted: 20 July 2010
© ISS 2010

Abstract

Objectives Our purpose was to identify imaging characteristics of tenosynovial and bursal chondromatosis.

Materials and methods We retrospectively reviewed 25 pathologically confirmed cases of tenosynovial ($n=21$) or bursal chondromatosis ($n=4$). Patient demographics and clinical presentation were reviewed. Imaging was evaluated by two musculoskeletal radiologists with agreement by consensus, including radiography ($n=21$), bone scintigraphy ($n=1$), angiography ($n=1$), ultrasonography ($n=1$), CT ($n=8$), and MR ($n=8$). Imaging was evaluated for lesion

location/shape, presence/number of calcifications, evidence of bone involvement, and intrinsic characteristics on ultrasonography/CT/MR.

Results Average patient age was 44 years (range 7 to 75 years) with a mild male predilection (56%). A slowly increasing soft tissue mass was the most common clinical presentation (53%). Lesion locations included the foot ($n=8$), hand ($n=6$), shoulder ($n=3$), knee ($n=2$), ankle ($n=2$) and one each in the upper arm, forearm, wrist, and cervical spine. All lesions were located in a known tenosynovial (21 cases, 84%) or bursal (four cases, 16%) location. All cases of bursal chondromatosis were round/oval in shape. Tenosynovial lesions were fusiform (65%) or round/oval (35%). Radiographs commonly showed a soft tissue mass (86%) and calcification (90%). Calcifications were predominantly chondroid (79%) or osteoid (11%) in character with >10 calcified bodies in 48%. CT detected calcifications in all cases. The intrinsic characteristics of the nonmineralized component showed low attenuation on CT (75%), high signal intensity on T2-weighted MR (76%) and a peripheral/septal contrast enhancement pattern (100%).

Conclusions Imaging of tenosynovial and bursal chondromatosis is often characteristic with identification of multiple osteochondral calcifications (90% by radiographs; 100% by CT). CT and MR also revealed typical intrinsic characteristics of chondroid tissue and lesion location in a known tendon sheath or bursa.

The opinions or assertions contained herein are the private views of the authors and are not to be construed as official or as reflecting the views of the Departments of the Army, Navy, or Defense.

M. D. Murphey
Department of Radiologic Pathology,
Armed Forces Institute of Pathology,
6825 16th Street NW, Building 54, Room M-133A,
Washington, DC 20306, USA

J. F. Fetsch
Department of Soft Tissue Pathology,
Armed Forces Institute of Pathology,
6825 16th Street NW, Building 54, Room M-133A,
Washington, DC 20306, USA

E. A. Walker · M. D. Murphey
Department of Radiology and Nuclear Medicine,
Uniformed Services University of the Health Sciences,
Bethesda, MD, USA

E. A. Walker (✉)
Department of Radiology, Milton S. Hershey Medical Center,
Hershey, PA, USA
e-mail: ewalker@hmc.psu.edu

Keywords Tenosynovial chondromatosis · Bursal chondromatosis · Chondroid neoplasm · Histology · Imaging

Report Documentation Page

Form Approved
OMB No. 0704-0188

Public reporting burden for the collection of information is estimated to average 1 hour per response, including the time for reviewing instructions, searching existing data sources, gathering and maintaining the data needed, and completing and reviewing the collection of information. Send comments regarding this burden estimate or any other aspect of this collection of information, including suggestions for reducing this burden, to Washington Headquarters Services, Directorate for Information Operations and Reports, 1215 Jefferson Davis Highway, Suite 1204, Arlington VA 22202-4302. Respondents should be aware that notwithstanding any other provision of law, no person shall be subject to a penalty for failing to comply with a collection of information if it does not display a currently valid OMB control number.

1. REPORT DATE

JUL 2010

2. REPORT TYPE

3. DATES COVERED

00-00-2010 to 00-00-2010

4. TITLE AND SUBTITLE

Imaging characteristics of tenosynovial and bursal chondromatosis

5a. CONTRACT NUMBER

5b. GRANT NUMBER

5c. PROGRAM ELEMENT NUMBER

6. AUTHOR(S)

5d. PROJECT NUMBER

5e. TASK NUMBER

5f. WORK UNIT NUMBER

7. PERFORMING ORGANIZATION NAME(S) AND ADDRESS(ES)

Armed Forces Institute of Pathology, Department of Radiologic Pathology, 6825 16th Street NW, Building 54, Room M-133A, Washington, DC, 20306

8. PERFORMING ORGANIZATION REPORT NUMBER

9. SPONSORING/MONITORING AGENCY NAME(S) AND ADDRESS(ES)

10. SPONSOR/MONITOR'S ACRONYM(S)

11. SPONSOR/MONITOR'S REPORT NUMBER(S)

12. DISTRIBUTION/AVAILABILITY STATEMENT

Approved for public release; distribution unlimited

13. SUPPLEMENTARY NOTES

14. ABSTRACT

Objectives Our purpose was to identify imaging characteristics of tenosynovial and bursal chondromatosis. **Materials and methods** We retrospectively reviewed 25 pathologically confirmed cases of tenosynovial (n=21) or bursal chondromatosis (n=4). Patient demographics and clinical presentation were reviewed. **Imaging** was evaluated by two musculoskeletal radiologists with agreement by consensus, including radiography (n=21), bone scintigraphy (n=1), angiography (n=1), ultrasonography (n=1), CT (n=8), and MR (n=8). Imaging was evaluated for lesion location/shape, presence/number of calcifications, evidence of bone involvement, and intrinsic characteristics on ultrasonography/CT/MR. **Results** Average patient age was 44 years (range 7 to 75 years) with a mild male predilection (56%). A slowly increasing soft tissue mass was the most common clinical presentation (53%). Lesion locations included the foot (n=8), hand (n=6), shoulder (n=3) knee (n=2), ankle (n=2) and one each in the upper arm forearm, wrist, and cervical spine. All lesions were located in a known tenosynovial (21 cases, 84%) or bursal (four cases, 16%) location. All cases of bursal chondromatosis were round/oval in shape. Tenosynovial lesions were fusiform (65%) or round/oval (35%). Radiographs commonly showed a soft tissue mass (86%) and calcification (90%). Calcifications were predominantly chondroid (79%) or osteoid (11%) in character with >10 calcified bodies in 48%. CT detected calcifications in all cases. The intrinsic characteristics of the nonmineralized component showed low attenuation on CT (75%), high signal intensity on T2-weighted MR (76%) and a peripheral/ septal contrast enhancement pattern (100%). **Conclusions** Imaging of tenosynovial and bursal chondromatosis is often characteristic with identification of multiple osteochondral calcifications (90% by radiographs; 100% by CT). CT and MR also revealed typical intrinsic characteristics of chondroid tissue and lesion location in a known tendon sheath or bursa.

15. SUBJECT TERMS

16. SECURITY CLASSIFICATION OF:			17. LIMITATION OF ABSTRACT Same as Report (SAR)	18. NUMBER OF PAGES 9	19a. NAME OF RESPONSIBLE PERSON
a. REPORT unclassified	b. ABSTRACT unclassified	c. THIS PAGE unclassified			

Standard Form 298 (Rev. 8-98)
Prescribed by ANSI Std Z39-18

Introduction

Primary synovial chondromatosis represents an uncommon benign neoplastic process with formation of hyaline cartilage nodules in the subsynovial tissue of a joint, tendon sheath, or bursa. The most common subtype of this disease involves the synovium of a joint. The term synovial osteochondromatosis is frequently used for this entity, but does not accurately reflect the pathologic characteristics as endochondral ossification of the cartilage nodules is not always present. A prior study by Davis and co-workers [1] demonstrated ossification was histologically absent in 45% of cases. This terminology is reflected by the use of the term synovial chondromatosis for this lesion by the World Health Organization.

Tenosynovial and bursal chondromatosis, which are histologically similar to the intraarticular counterpart, arise from the synovium of the tendon sheath or bursa, respectively. Tenosynovial chondromatosis is much less common than the intraarticular form of this disease and most frequently affects the hands and feet [2, 3]. Bursal chondromatosis is rare and not well described in the literature. Similar to the intraarticular form of the disease, both tenosynovial and bursal chondromatosis may have cellular atypia that can be misinterpreted as chondrosarcoma histologically if the synovial origin is not recognized [4, 5].

There are only limited descriptions of the radiologic appearance of tenosynovial and bursal chondromatosis. Our purpose was to describe the imaging appearance of the largest series to date with pathologic correlation.

Materials and methods

We retrospectively reviewed 25 cases of pathologically confirmed tenosynovial ($n=21$) or bursal chondromatosis ($n=4$) from the archives of the Armed Forces Institute of Pathology collected between 1978 and 2009. This study was performed with the approval of the Armed Forces Institute of Pathology Human Subjects Committee in compliance with the Health Insurance Portability and Accountability Act (HIPPA). Informed consent was not required. Criteria for inclusion in the study were (1) imaging studies of adequate quality available for review (radiographs, angiography, bone scintigraphy, CT or MR imaging) and (2) pathologic diagnosis of synovial chondromatosis with imaging and/or surgical report demonstrating a tenosynovial or bursal location.

Radiologic studies were reviewed by two musculoskeletal radiologists (E.A.W. and M.D.M.) with complete knowledge of the pathologic findings and agreement of the findings was by consensus and included radiographs ($n=21$), angiography

($n=1$), bone scintigraphy ($n=1$), ultrasonography (US) ($n=1$), CT ($n=8$), and MR imaging ($n=8$).

Evaluation included patient demographics (patient sex and age) and clinical symptoms at presentation, if available. Lesion size (including size range and average) was determined by the shortest and longest axis by the best imaging modality depicting the mass. Possible lesion locations included the foot, hand, shoulder, knee, forearm, wrist, upper arm, ankle, and spine (cervical, thoracic, or lumbar) (Table 1). When a tenosynovial lesion involved the hands, wrists, or feet, it was noted whether the lesion was volar/plantar or dorsal in location. Lesion location (tendon sheath or bursa involved) was determined by the best imaging modality depicting the mass in correlation with the surgical report (when available). The lesion shape was characterized as fusiform or round/oval for both tenosynovial and bursal locations determined by the best imaging modality depicting the tumor.

Radiographs ($n=21$)

The presence of a soft tissue mass or fullness was determined radiographically. Lesions were evaluated for the presence of calcification. If present, the extent (mild, moderate, or marked {mild mineralization is defined as mineralization extending through less than one-third of the lesion, moderate mineralization involves greater than one-third and less than two-thirds of the lesion, marked mineral extends through greater than two-thirds of the lesion}) and predominant character [chondroid (ring and arc appearance), osteoid (dense ivory appearance), or nonspecific] of the calcification was determined. The number of distinct calcified cartilaginous bodies detected was quantified as 0, 1–4, 5–10, or greater than 10. Radiographs were also evaluated for the presence of bone erosion, bone invasion, and periosteal reaction. If periosteal reaction was present, its character was determined as an aggressive or nonaggressive pattern.

Scintigraphy ($n=1$) and angiography ($n=1$)

Bone scintigraphy (blood flow, blood pool, and static images) was evaluated for the degree of radionuclide uptake (none, mild, moderate, marked {mild uptake is defined as less than the anterior iliac spines on whole body bone scan, moderate uptake is defined as equal to the anterior iliac spines on whole body bone scan, marked uptake is defined as greater than the anterior iliac spines on whole body bone scan}), homogeneity or heterogeneity and if the latter, the presence of central photopenia (donut sign). Angiography was evaluated for the presence of tumor staining (avascular, hypovascular, or hypervascular), the degree (mild, moderate, or marked) and pattern (diffuse or

Table 1 Patient characteristics showing case number, patient age, sex (M or F), tenosynovial versus bursal chondromatosis (T or B), and location of the lesion

Case no.	Age	Sex	T/B	Location
1	65	F	T	Leg biceps tendon knee
2	52	M	T	Wrist and forearm flexor tendon sheath
3	46	M	B	Bursae beneath pectoralis major muscle
4	46	M	T	Flexor tendon sheath phalanges 5th finger
5	36	F	T	Extensor tendon sheath 2nd metatarsal
6	32	F	T	Biceps tendon sheath shoulder
7	65	F	T	Extensor tendon sheath distal phalanx 5th finger
8	46	F	T	Dorsal forearm
9	55	F	T	Dorsal to talonavicular joint
10	36	M	B	Spine - Arch of C1
11	75	F	T	Flexor tendon sheath proximal phalanx 5th toe
12	47	M	T	Ankle
13	59	M	T	Flexor tendon sheath 5th finger
14	69	F	T	Flexor tendon sheath 1st metacarpal
15	28	F	T	Flexor tendon sheath 2nd MCP joint foot
16	22	M	T	Flexor tendon sheath 5th metatarsal head
17	26	M	T	Flexor tendon sheath 2nd metatarsal
18	48	M	B	Posterior medial femoral metaphysis knee
19	29	F	T	Upper arm
20	59	M	T	Flexor tendon sheath proximal phalanx 2nd finger
21	46	M	T	Biceps tendon sheath shoulder
22	49	M	T	Flexor tendon sheath proximal phalanx thumb
23	13	M	B	Plantar heel
24	41	M	T	Flexor hallucis longus tendon sheath ankle and hindfoot
25	7	F	T	Extensor digitorum longus tendon sheath ankle

peripheral) of tumor blush. The presence or absence of arteriovenous shunting, early draining veins, and displacement of native vessels were also determined.

Sonography (US) ($n=1$)

The lesion margin was determined to be: defined with a pseudocapsule (complete echogenic rim), defined with a partial pseudocapsule (partial echogenic rim), defined without a pseudocapsule, or with an infiltrative border (ill-defined margin). The predominant echogenicity of the lesion was characterized as anechoic, hypoechoic, or hyperechoic. The lesion was also evaluated for homogeneity or heterogeneity. The presence or absence of hyperechoic foci with shadowing resulting from mineralization was also evaluated.

Computed Tomography (CT) ($n=8$)

CT scans were performed with axial images of 3–10 mm thickness with both bone and/or soft tissue windows available for review. Lesion margins were evaluated as defined with a pseudocapsule (complete high attenuation rim), defined with a partial pseudocapsule (partial high

attenuation rim), defined without a pseudocapsule or infiltrative border. CT examinations were evaluated for the presence of calcification. If present, the extent (mild, moderate, or marked {mild mineralization is defined as mineralization extending through less than one-third of the lesion, moderate mineralization involves greater than one-third and less than two-thirds of the lesion, marked mineral extends through greater than two-thirds of the lesion}) and predominant character [chondroid (ring and arc appearance), osteoid (dense ivory appearance) or nonspecific] of the calcification was determined. The presence of a rim of fat or fat within the lesion was determined. The bone adjacent to the lesion was evaluated for bone erosion, bone invasion, or periosteal reaction. If periosteal reaction was present, the character was described as aggressive or nonaggressive. CT images were evaluated for the predominant tissue attenuation (lower than muscle, similar to muscle, or higher than muscle) and tissue homogeneity or heterogeneity of the nonmineralized component of the lesion. CT following intravenous contrast administration was evaluated for the degree (mild, moderate, or marked) and pattern (peripheral, septal, nodular, diffuse, or any combination) of enhancement. CT was evaluated for hemorrhage (low attenuation with rim enhancement and

fluid levels) or central necrosis (low attenuation with rim enhancement). The presence of joint invasion (tumor extending into an articulation) or neurovascular encasement (tumor surrounding greater than 50% of a major neurovascular bundle) was also determined by CT.

Magnetic Resonance (MR) imaging ($n=8$)

MR imaging was performed with various high field units (1.0–1.5 T). MR imaging sequences available for review included standard (spin echo) T1-weighting (TE 480–800 ms; TR 14–30 ms) ($n=8$) and T2-weighting (TR 1,800–4,100 ms; TE 70–119 ms) ($n=8$), and post-gadolinium injection T1-weighted sequences ($n=3$). Lesion margin was evaluated as defined with a pseudocapsule (complete border with higher T1 and lower T2 signal than the lesion), defined with a partial pseudocapsule (partial border with higher T1 and lower T2 signal than the lesion), defined without a pseudocapsule or infiltrative border. Foci of low signal on all pulse sequences were evaluated as present or absent. These areas were then correlated with radiographs or CT (if available) to determine if they corresponded to areas of mineralized matrix. When present, these foci of low signal were characterized as subtle or obvious and small, moderate or large in extent. The lesion was evaluated for fatty rim or internal fat. The bone adjacent to the lesion was evaluated for bone erosion, marrow invasion, and periosteal reaction (high signal intensity on the bone surface on long TR sequences). MR images were evaluated for the predominant signal intensity on each sequence as follows: 1. On T1-weighted images, lesions were characterized as less than muscle (low signal intensity), similar to muscle (intermediate signal intensity), or greater than muscle approaching the signal of fat (high signal intensity); 2. On T2-weighted sequences, lesions were characterized as similar to muscle (low signal intensity), higher than muscle to similar to fat (intermediate signal intensity), greater than fat (mild high signal intensity) or equal to water (marked high signal intensity). The lesion was evaluated for homogeneity or heterogeneity on both T1-weighted and T2-weighted MR images. MR images following intravenous contrast administration were evaluated for the degree (mild, moderate, or marked) and pattern (peripheral, septal, nodular, diffuse, or any combination) of enhancement. MR was evaluated for hemorrhage (foci of high signal intensity on all pulse sequences or fluid levels with rim enhancement following intravenous contrast if available) or central necrosis (low signal on T1, high signal on T2 with rim enhancement following intravenous contrast if available). The presence of joint invasion (tumor extending into an articulation) or neurovascular encasement (tumor surrounding greater than 50% of a major neurovascular bundle) was also determined by MR imaging.

Results

Of the 25 cases of chondromatosis, 14 were male (56%) and 11 were female (44%). The patients ranged in age from 7 to 75 years with an average age of 44 years. History of presenting symptoms was available in 17 of the 25 patients. A mass slowly increasing in size was reported in nine patients (53%). Pain was the presenting symptom in seven patients (41%). Swelling was present in five of the 17 patients (29%). In two patients (12%), the lesion was an incidental finding. A single patient (6%) presented with a decreased range of motion and one patient (6%) reported numbness. The average lesion size was 3.9×1.7 cm with a range from 1.0×0.3 cm to 16.0×2.3 cm. Lesion locations included eight in the foot (32%), six in the hand (24%), three in the shoulder (12%), two in the knee (8%), two in the ankle (8%), and one each (4%) in the upper arm, forearm, wrist, and cervical spine. Of the hand and wrist tenosynovial lesions, six of seven (86%) were located volar. Of eight foot tenosynovial lesions, five were plantar (63%) and three were dorsal (37%). Correlation of cross-sectional imaging and surgical reports identified that all lesions were located in a known tenosynovial (21 cases, 84%) or bursal (four cases, 16%) location. All cases of bursal chondromatosis were round or oval in shape. The shape could be determined in 20 of the tenosynovial lesions, 13 were fusiform (65%) and seven were round or oval (35%).

Radiographs

A soft tissue mass or fullness was identified in 18 (86%) of the 21 cases with radiographs. Mineralization was demonstrated in 19 (90%) cases while two (10%) lesions were noncalcified (Figs. 1 and 2). The extent of calcification was mild in four cases (21%), moderate in eight lesions (42%), and marked (37%) in seven cases. The predominant character of the calcification was chondroid in 15 (79%) of lesions (Figs. 1 and 2), osteoid in two cases (11%), and nonspecific in two cases (10%). The number of distinct cartilaginous bodies detected on radiographs was greater than ten in ten cases (48%), 5–10 in two cases (10%), 1–4 in seven cases (33%) or no distinct cartilaginous bodies in two cases (9%). Bone erosion occurred in nine cases (43%). No bone invasion or periosteal reaction was identified on radiographs.

Bone scintigraphy and angiography

Bone scintigraphic images of the single case evaluated included blood pool and static images. On blood pool images, there was marked and homogeneous uptake of radiotracer. Static images demonstrate mild heterogeneous uptake. Angiography in this case revealed mild hyper-

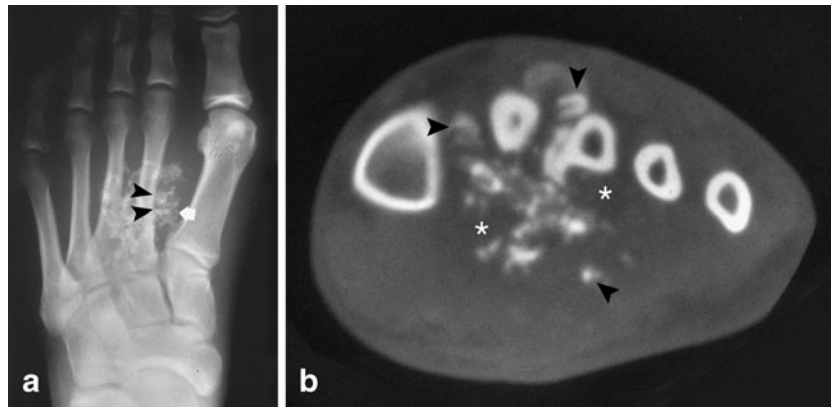


Fig. 1 Tenosynovial chondromatosis centered in the flexor tendon sheath of the foot of a 26-year-old male with pain and slowly growing soft tissue mass. **a** Radiograph showing multiple predominantly chondroid foci of matrix mineralization (*white arrow*) and extrinsic erosion (*black arrowheads*) of the underlying metatarsal. **b** CT also

reveals multiple predominantly chondroid foci of matrix mineralization (*black arrowheads*). There is low attenuation of the nonmineralized chondroid tissue (*). Both imaging studies show oval morphology of the lesion

vascularity with a diffuse pattern. There was no arteriovenous shunting or early draining veins. There was mild displacement of native vessels caused by the mass.

Sonography (US)

The single case with sonographic evaluation revealed a defined margin with a partial pseudocapsule. The lesion was predominantly hypoechoic and contained multiple small hyperechoic foci with shadowing resulting from mineralization (Fig. 3).

Computed Tomography (CT)

Of the eight CT examinations, lesion margins were defined with a pseudocapsule in two patients (25%), defined with a partial pseudocapsule in five cases (62%) and defined without a pseudocapsule in one case (13%). Mineralization was seen in all eight cases (Figs. 1 and 3). The extent of mineralization was characterized as mild in one (12%), moderate in three (38%) cases, and marked in four (50%) cases. The predominant character of mineralization was chondroid in six cases (75%) (Figs. 1, 3, and 4) and osteoid in two cases (25%). There was no evidence of a rim of fat or fat within any lesion. Bone erosion was present in six cases (75%) on CT, but no bone invasion was seen. Periosteal reaction was present in one case (12%) and was nonaggressive in character (Fig. 4). The predominant attenuation of the nonmineralized portion of the lesion was less than muscle in six cases (75%) (Fig. 1) and similar to muscle in two cases (25%). Lesion attenuation was heterogeneous in six cases (75%) and homogeneous in two lesions (25%). Of the eight lesions imaged by CT, only one received intravenous contrast and enhancement was peripheral and septal. No evidence of hemorrhage, central

necrosis, joint invasion, or neurovascular encasement was seen.

Magnetic Resonance (MR) imaging

Of the eight MR examinations, lesion margins were defined with a pseudocapsule in six cases (75%), and defined with a partial pseudocapsule in two lesions (25%). Foci of low signal on all pulse sequences were seen in six of eight cases (75%) and correlated with mineralized matrix on available radiographs and/or CT examinations in all cases (Figs. 2, 4, and 5). The low signal intensity was obvious in five cases (83%), and subtle in one lesion (17%). The low signal intensity extent was small in two cases (33%), moderate in three lesions (50%), and large in one case (17%). A small rim of fat was seen about two lesions (25%) and two cases (25%) contained fat within the lesion, which correlated to yellow marrow within osteochondral bodies. Bone erosion was identified in two lesions (25%), but no marrow invasion or periosteal reaction was seen. On T1-weighted MR sequences, the predominant signal was similar to muscle (intermediate signal intensity) in all cases (Figs. 4 and 5). On T2-weighted MR sequences, the predominant signal intensity was intermediate (higher than muscle to similar to fat) in two cases (24%), mildly high signal intensity (greater than fat) in three cases (38%) and marked high signal intensity (equal to water) in three lesions (38%) (Fig. 4). Lesion signal intensity was heterogeneous in all cases on T1-weighted and T2-weighted MR sequences. In all three cases evaluated following intravenous gadolinium, there was mild enhancement with a peripheral and septal pattern (Figs. 2 and 5). No lesions revealed hemorrhage, central necrosis, joint invasion, or neurovascular encasement.

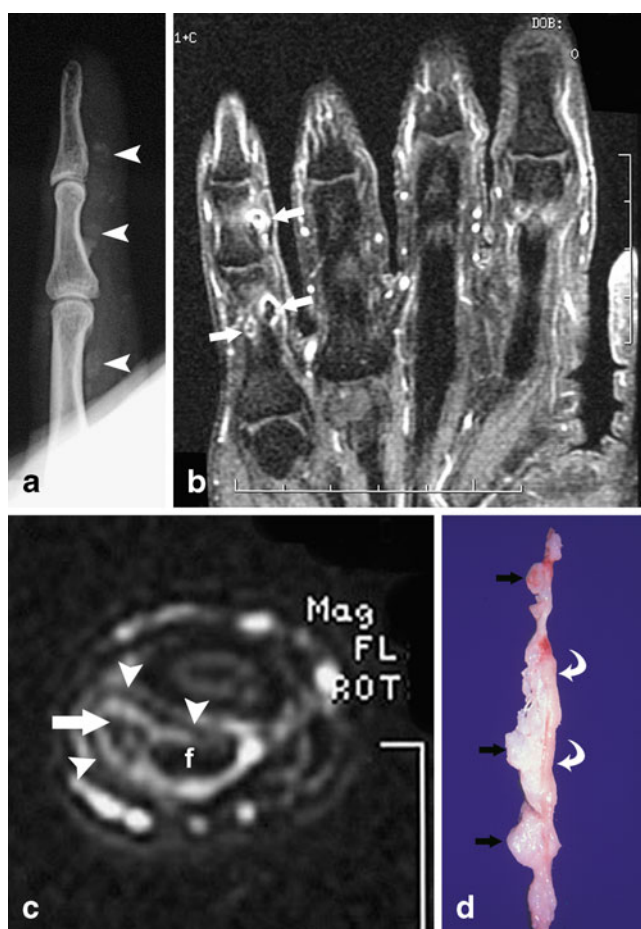


Fig. 2 Tenosynovial chondromatosis involving the flexor tendon sheath of the fifth digit in a 46-year-old male with slowly growing soft tissue mass over 8 months. **a** Lateral radiograph showing chondroid mineralization palmar to the fifth finger (*white arrowheads*) with typical fusiform morphology. **b** MR coronal post-contrast T1 fat-saturation image (TR/TE 416/13) with peripheral enhancement about the chondral bodies (*white arrows*). **c** Axial T2 fat-saturation image (TR/TE 4,316/103) showing high signal intensity peripherally and low signal centrally (*white arrow*) representing a mineralized focus intimately related to the flexor tendon (**f**) and within the tendon sheath (*white arrowheads*). **d** Resected gross specimen reveals chondroid nodules (*black arrows*) and tendon (*curved arrows*)

Discussion

Tenosynovial and bursal chondromatosis are two manifestations of cartilaginous lesions arising from neoplasia of the synovial membrane. This process is similar to the more common intraarticular form of the disease, which has been extensively described in the literature, but affects the synovium of the tendon sheath or bursa [6–9]. However, there are only limited descriptions of the radiologic appearance of tenosynovial and bursal chondromatosis. These lesions may show considerable cellular atypia leading to histologic misinterpretation as chondrosarcoma if the pathologist uses the same criteria as for evaluating cartilage lesions of bone [10].

In our series of cases, there was a mild male predilection (56% of cases). The average patient age was in the fifth decade, and there were only two patients under 20 years of age. When clinical history was available, the most common presenting clinical symptom was a soft tissue mass slowly increasing in size reported in nine of 17 (53%) of our cases. Pain was a presenting feature in seven of 17 (41%) of cases. Swelling (29%), decreased range of motion (6%), and numbness (6%), were seen less frequently. Clinical symptoms and average age were similar to previous reports [11, 12].

Tenosynovial chondromatosis, similar to previous reports, shows a strong predilection for the hands or feet [3, 5, 10, 12–14]. Of our 21 cases of tenosynovial chondromatosis, seven (33%) were located in the hands/wrist and ten (48%) involve the feet/ankle. The hand/wrist lesions were most frequently volar (86%), which correlates with previously reported data in the literature [15]. Patel and coworkers hypothesize that the limited dorsal involvement in the hand may be related to the absence of a synovial sheath and therefore a paucity of synovial cells about these extensor tendons [11]. Foot tenosynovial lesions were more equally distributed with five plantar (63%) and three dorsal (37%).

Tenosynovial and bursal chondromatosis have many imaging features similar to intraarticular synovial chondromatosis as well as other chondroid lesions. Presence of mineralization was important to suggest the diagnosis of tenosynovial or bursal chondromatosis. On radiographs, 90% of lesions demonstrated mineralization. As expected, CT was superior in detecting matrix mineralization, which was seen in 100% of cases and was moderate to marked in extent in 88% of lesions. The character of mineralization was predominantly chondroid (75% on CT, 79% on radiographs). Osteoid matrix mineralization predominated less frequently (25% on CT, 11% on radiographs). The number of distinct osteochondral bodies was greater than ten in 48% of cases evaluated by radiograph.

In our opinion, lesion shape and location was important to suggest the diagnosis of tenosynovial chondromatosis in comparison to other diagnostic considerations. The majority of tenosynovial lesions in our series (65%) revealed a fusiform morphology conforming to the shape of the involved tendon sheath (Figs. 2 and 4). The remaining 35% of tenosynovial lesions demonstrated a round or oval shape (Fig. 1). As expected, all bursal lesions in our series showed a round or oval morphology (Figs. 3 and 5). Cross-sectional imaging detected a location within a known tenosynovial sheath or bursa in all cases. Because of the superior contrast resolution of MR, this modality optimally depicts the specific tendon or bursa affected.

CT attenuation of the nonmineralized portion of the lesion was less than skeletal muscle in 75% of the lesions reflecting the high water content seen in hyaline cartilage



Fig. 3 Subcoracoid bursal chondromatosis in a 46-year-old male complaining of pain, decreased range of motion, and slowly growing soft tissue mass. **a** Axial CT demonstrating multiple calcified chondroid bodies (*white arrowheads*) within the subcoracoid bursa. Radiographs (not shown) did not reveal any calcification. **b**

Ultrasound image showing multiple echogenic foci (*white arrows*) with shadowing (*white open arrowheads*). **c** A gross specimen with bursal lining (*curved black and white arrow*) and multiple chondroid bodies (*black arrows*)

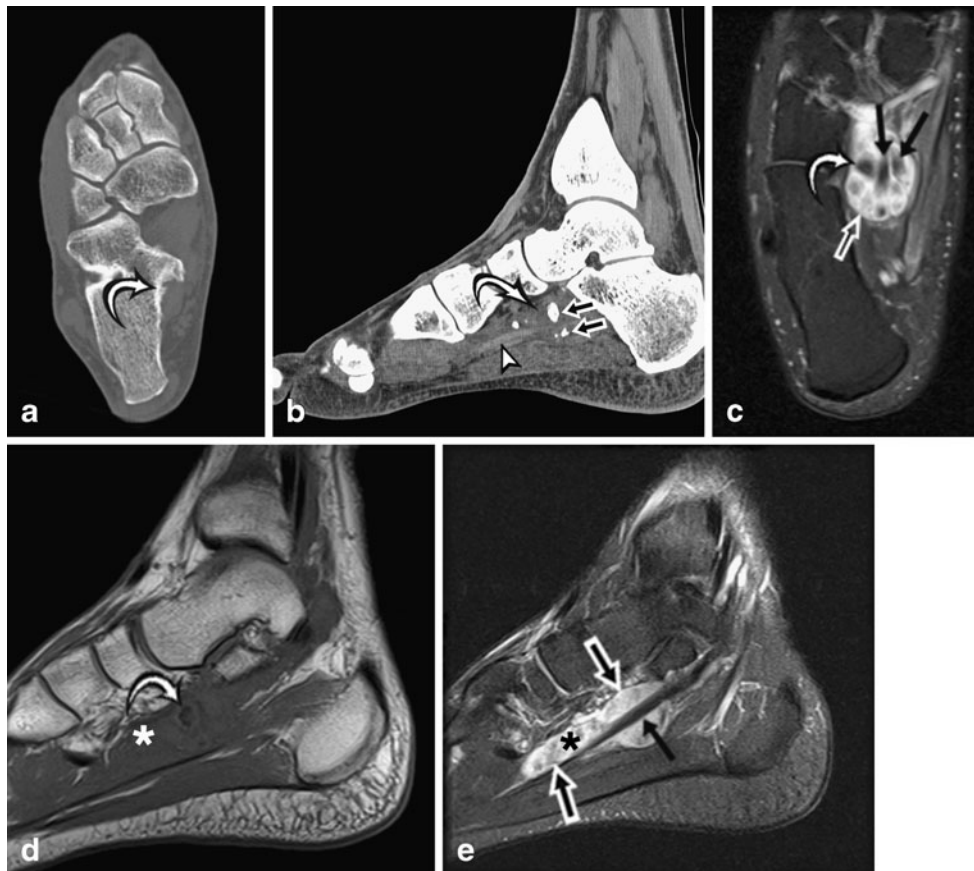


Fig. 4 Tenosynovial chondromatosis involving the flexor hallucis longus (FHL) tendon sheath in a 41-year-old man discovered during evaluation for a lower tibial stress fracture. **a** Long axis CT (*bone windows*) demonstrates extrinsic erosion and mild periosteal reaction (*curved arrow*). **b** Sagittal CT (*soft tissue windows*) shows the lesion surrounding the FHL tendon (*white in black arrowhead*) with attenuation less than skeletal muscle (*white in black curved arrow*) and multiple mineralized foci (*small black in white arrows*). **c**, **d**, **e** Long axis T2 fat-suppressed (FS) (*c-TR/TE 5,257/60.6*), sagittal T1

(*d-TR/TE 625/9.7*) and sagittal PDFS (*e-TR/TE 2042/67.9*) MR images reveal the fusiform chondroid lesion (*small black in white arrows*) surrounding the FHL and flexor digitorum longus tendons (*black arrows*) at the master knot of Henry. Foci of mineralization are low signal intensity on all pulse sequences (*curved white in black arrows*) is noted within the high signal chondroid tissue. Non-mineralized chondroid regions are intermediate signal on T1 (**d**) and high signal intensity on long TR images (**e-***)

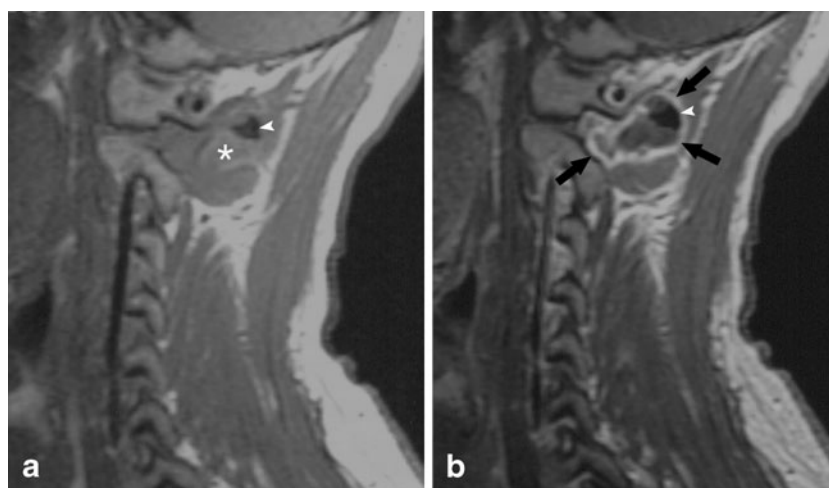


Fig. 5 Bursal chondromatosis involving the cervical spine in a 36-year-old male presenting with arm numbness demonstrates oval morphology. **a, b** Sagittal T1-weighted MR images before (a-TR/TE 550/16) and following intravenous gadolinium (TR/TE 550/14) showing the oval morphology of the soft tissue mass between the C1 and C2 posterior

elements. There is predominantly intermediate signal on T1-weighting (*) and peripheral and septal enhancement after contrast (*black arrows*). Persistent low signal intensity region (*white arrowheads*) corresponding to calcification on CT (not shown). Pathology revealed synovial lining representing interspinous bursa (not shown)

neoplasms [16, 17]. Similar to CT, high-water-content cartilaginous tissue is demonstrated as high signal intensity on T2-weighted MR sequences in 76% of cases. Peripheral and septal enhancement is characteristically seen in cartilaginous lesions on post-contrast MR images caused by the vascularized fibrous pseudocapsule and fibrous connective tissue between the cartilage lobules. This MR pattern of enhancement was seen in all three of our cases after contrast administration.

Differential diagnosis for tenosynovial and bursal chondromatosis lesions includes synovial chondromatosis, soft tissue/periosteal chondroma, calcifying aponeurotic fibroma, bizarre parosteal osteochondromatous proliferation (BPOP, Nora Lesion), and the focal form of pigmented villonodular synovitis (PVNS), which is also referred to as giant cell tumor of tendon sheath (GCTTS). In addition, two malignant lesions, synovial sarcoma and extraskeletal chondrosarcoma, should also be considered. The majority of these diagnostic possibilities can be excluded by lesion location and morphology. Synovial chondromatosis rarely affects the hand or foot and is distinguished from tenosynovial or bursal chondromatosis by its intraarticular location. Intrinsic characteristics of these lesions are identical, reflecting their underlying pathology.

Distinguishing between tenosynovial chondromatosis and soft tissue/periosteal chondroma can be difficult. These lesions show similar patient demographics, anatomic distribution, and frequently present as a soft tissue mass near a tendon sheath [18, 19]. These lesions also have similar matrix mineralization on radiography and CT. The key to distinguishing these entities is the identification of the lesion adjacent to but not in a tendon sheath or typical

bursal location on cross-sectional imaging with soft tissue/periosteal chondroma. In addition, tenosynovial chondromatosis typically demonstrates a fusiform shape with multiple distinct and separable nodules whereas soft tissue/periosteal chondromas are more commonly round or ovoid [17]. Differentiating these two lesions is important for determining the likelihood of recurrence. Tenosynovial chondromatosis is much more likely to locally recur (38–88%) [2]. This is in contradiction to soft tissue chondroma, which has a significantly lower local recurrence rate of 18% [19].

Calcifying aponeurotic fibroma is a rare fibroblastic lesion with a notable tendency for local recurrence, most commonly affecting the palms of the hands and soles of the feet in young children. It has a peak incidence in the first decade, the average patient being much younger than patients with tenosynovial chondromatosis. Cartilage nodules range from 0 to 30% of tumor volume and may show a fine stippling of focal calcification and therefore may simulate tenosynovial chondromatosis on radiographs [20]. However, on cross-sectional imaging, calcifying aponeurotic fibroma are juxtaposed, but not within the tendon sheath. In addition, on MR imaging these lesions reveal lower signal intensity on T2-weighting and diffuse gadolinium enhancement in contrast to tenosynovial chondromatosis [21].

Bizarre parosteal osteochondromatous proliferation (BPOP) is a rare lesion that is typically seen in young adults with an age range of 14–74 years of age. This lesion usually affects the hands and feet, similar to tenosynovial chondromatosis. BPOP arises and is attached to the cortical surface of the underlying bone, and may encompass an adjacent tendon sheath. However, BPOP is not centered within a tendon sheath. In contradistinction, tenosynovial

chondromatosis is distinctly separate from the adjacent cortex and on cross-sectional imaging is within a tendon sheath [22].

The focal form of PVNS or GCTTS frequently affects a tendon sheath of the hand or foot [23]. Intralesional calcifications are unusual but have been reported in up to 5.5% of cases, mimicking tenosynovial chondromatosis [24, 25]. However, MR imaging of GCTTS reveals lower signal intensity on T2-weighting related to hemosiderin deposition (blooming artifact may also be present on gradient echo sequences) and diffuse gadolinium enhancement in contrast to tenosynovial chondromatosis [23, 26].

Synovial sarcoma may calcify in 30% of cases and frequently affects the foot and ankle (18% of cases) [27]. Mineralization is commonly peripheral or eccentric, but the character of the calcification is not chondroid. Cross-sectional imaging frequently demonstrates marked heterogeneity, hemorrhage, and fluid levels, features not seen in cartilaginous lesions [27]. In addition, while the lesions can engulf tendons, they are not centered in a bursa or in a tendon sheath.

Extraskeletal chondrosarcoma is uncommon, most frequently involves the thigh, and only rarely affects the hands and feet. While chondroid mineralization and intrinsic characteristics could simulate features seen with tenosynovial and bursal chondromatosis, extraskeletal chondrosarcomas are not located within a bursa or tendon sheath on cross-sectional imaging and typically reveal additional aggressive features (large size, heterogeneity, hemorrhage) [17].

In conclusion, tenosynovial or bursal chondromatosis demonstrates calcification in the vast majority of cases. The intrinsic characteristics on CT or MR imaging reveal the typical high-water-content features of hyaline cartilage neoplasms. Fusiform shape of a calcified soft tissue lesion, particularly in the hands or feet, may suggest the diagnosis of tenosynovial chondromatosis. However, in addition to these imaging features, the specific diagnosis of tenosynovial or bursal chondromatosis can be confirmed by the lesion location within a known bursa or tendon sheath, which is optimally depicted by MR imaging.

Acknowledgment The authors gratefully acknowledge the residents who attend the AFIP radiologic pathology courses (past, present, and future) for their contribution to our series of patients.

Conflict of interest The authors declare that they have no conflicts of interest.

References

- Davis RI, Hamilton A, Biggart JD. Primary synovial chondromatosis: a clinicopathologic review and assessment of malignant potential. *Hum Pathol.* 1998;29(7):683–8.
- Dahlin DC, Salvador AH. Cartilaginous tumors of the soft tissues of the hands and feet. *Mayo Clin Proc.* 1974;49(10):721–6.
- Fetsch JF, et al. Tenosynovial (extraarticular) chondromatosis: an analysis of 37 cases of an underrecognized clinicopathologic entity with a strong predilection for the hands and feet and a high local recurrence rate. *Am J Surg Pathol.* 2003;27(9):1260–8.
- Lichtenstein L, Goldman RL. Cartilage tumors in soft tissues particularly in the hand and foot. *Cancer.* 1964;17:1203–8.
- Sim FH, Dahlin DC, Ivins JC. Extra-articular synovial chondromatosis. *J Bone Joint Surg Am.* 1977;59(4):492–5.
- Murphey MD, et al. Imaging of synovial chondromatosis with radiologic-pathologic correlation. *Radiographics.* 2007;27(5):1465–88.
- Roberts D, Miller TT, Erlanger SM. Sonographic appearance of primary synovial chondromatosis of the knee. *J Ultrasound Med.* 2004;23(5):707–9.
- Villacin AB, Brigham LN, Bullough PG. Primary and secondary synovial chondrometaplasia: histopathologic and clinicoradiologic differences. *Hum Pathol.* 1979;10(4):439–51.
- Wittkop B, Davies AM, Mangham DC. Primary synovial chondromatosis and synovial chondrosarcoma: a pictorial review. *Eur Radiol.* 2002;12(8):2112–9.
- DeBenedetti MJ, Schwinn CP. Tenosynovial chondromatosis in the hand. *J Bone Joint Surg Am.* 1979;61(6A):898–903.
- Patel MR, Desai SS. Tenosynovial osteochondromatosis of the extensor tendon of a digit: case report and review of the literature. *J Hand Surg Am.* 1985;10(5):716–9.
- Someren A, Merritt WH. Tenosynovial chondroma of the hand: a case report with a brief review of the literature. *Hum Pathol.* 1978;9(4):476–9.
- Bui-Mansfield LT, Rohini D, Bagg M. Tenosynovial chondromatosis of the ring finger. *AJR Am J Roentgenol.* 2005;184(4):1223–4.
- Lynn MD, Lee J. Periarticular tenosynovial chondrometaplasia. Report of a case at the wrist. *J Bone Joint Surg Am.* 1972;54(3):650–2.
- Metha JA, Bignold LP, Pope RO. Intraarticular rupture of digital tenosynovial calcification: an unusual case of acute arthritis of the finger. *J Rheumatol.* 1999;26(7):1643–4.
- Cohen EK, et al. Hyaline cartilage-origin bone and soft-tissue neoplasms: MR appearance and histologic correlation. *Radiology.* 1988;167(2):477–81.
- Murphey MD, et al. From the archives of the AFIP: imaging of primary chondrosarcoma: radiologic-pathologic correlation. *Radiographics.* 2003;23(5):1245–78.
- Chung EB, Enzinger FM. Chondroma of soft parts. *Cancer.* 1978;41(4):1414–24.
- Weiss SW, Goldblum JR. Enzinger and Weiss's soft tissue tumors. In: Weiss SW, editor. *Cartilaginous soft tissue tumors.* 4th ed. St. Louis: Mosby; 2001. 1632.
- Fetsch JF, Miettinen M. Calcifying aponeurotic fibroma: a clinicopathologic study of 22 cases arising in uncommon sites. *Hum Pathol.* 1998;29(12):1504–10.
- Morii T, et al. Clinical significance of magnetic resonance imaging in the preoperative differential diagnosis of calcifying aponeurotic fibroma. *J Orthop Sci.* 2008;13(3):180–6.
- Torreggiani WC, et al. MR imaging features of bizarre parosteal osteochondromatous proliferation of bone (Nora's lesion). *Eur J Radiol.* 2001;40(3):224–31.
- Murphey MD, et al. Pigmented villonodular synovitis: radiologic-pathologic correlation. *Radiographics.* 2008;28(5):1493–518.
- Baker ND, et al. Pigmented villonodular synovitis containing coarse calcifications. *AJR Am J Roentgenol.* 1989;153(6):1228–30.
- Karasick D, Karasick S. Giant cell tumor of tendon sheath: spectrum of radiologic findings. *Skeletal Radiol.* 1992;21(4):219–24.
- Jelinek JS, et al. Giant cell tumor of the tendon sheath: MR findings in nine cases. *AJR Am J Roentgenol.* 1994;162(4):919–22.
- Murphey MD, et al. From the archives of the AFIP: imaging of synovial sarcoma with radiologic-pathologic correlation. *Radiographics.* 2006;26(5):1543–65.